Clinical, cellular, and neuropathological consequences of AP1S2 mutations: further delineation of a recognizable X-linked mental retardation syndrome

Guntram Borck, Anahi Mollà-Herman, Nathalie Boddaert, Ferechte Encha-Razavi, Anne Philippe, Laurence Robel, Isabelle Desguerre, Francis Brunelle, Alexandre R. Benmerah, Arnold Munnich, et al.

HUMAN MUTATION 29(7), 966–974, 2008

RESEARCH ARTICLE

Clinical, Cellular, and Neuropathological Consequences of *AP1S2* Mutations: Further Delineation of a Recognizable X-Linked Mental Retardation Syndrome

Guntram Borck,[1] Anahi Mollà-Herman,[6,7] Nathalie Boddaert,[2] Férechté Encha-Razavi,[3] Anne Philippe,[1] Laurence Robel,[4] Isabelle Desguerre,[5] Francis Brunelle,[2] Alexandre Benmerah,[6,7] Arnold Munnich,[1] and Laurence Colleaux[1]*

[1]INSERM U781 and Department of Medical Genetics, Hôpital Necker-Enfants Malades, Université Paris Descartes, Faculté de Médecine, Assistance Publique–Hôpitaux de Paris (AP-HP), Paris, France; [2]Department of Pediatric Radiology and INSERM U797, Hôpital Necker-Enfants Malades, Université Paris Descartes, Faculté de Médecine, Assistance Publique–Hôpitaux de Paris (AP-HP), Paris, France; [3]Department of Genetics, Embryo-Fetal Pathology Unit, Hôpital Necker-Enfants Malades, Université Paris Descartes, Faculté de Médecine, Assistance Publique–Hôpitaux de Paris (AP-HP), Paris, France; [4]Department of Child Psychiatry, Hôpital Necker-Enfants Malades, Université Paris Descartes, Faculté de Médecine, Assistance Publique–Hôpitaux de Paris (AP-HP), Paris, France; [5]Department of Neuropediatrics, Hôpital Necker-Enfants Malades, Université Paris Descartes, Faculté de Médecine, Assistance Publique–Hôpitaux de Paris (AP-HP), Paris, France; [6]INSERM, U567, Paris, France; [7]Institut Cochin, Université Paris Descartes, CNRS (UMR 8104), Paris, France.

Communicated by Andreas Gal

Mutations in the *AP1S2* gene, encoding the σ1B subunit of the clathrin-associated adaptor protein complex (AP)-1, have been recently identified in five X-linked mental retardation (XLMR) families, including the original family with Fried syndrome. Studying four patients in two unrelated families in which *AP1S2* nonsense and splice-site mutations segregated, we found that affected individuals presented, in addition to previously described features, with elevated protein levels in cerebrospinal fluid (CSF). Moreover, computed tomography scans demonstrated that the basal ganglia calcifications associated with *AP1S2* mutations appeared during childhood and might be progressive. Based on these observations, we propose that *AP1S2* mutations are responsible for a clinically recognizable XLMR and autism syndrome associating hypotonia, delayed walking, speech delay, aggressive behavior, brain calcifications, and elevated CSF protein levels. Using the AP-2 complex, in which the σ subunit is encoded by one single gene, as a model system, we demonstrated that σ subunits are essential for the stability of human AP complexes. By contrast, no major alteration of the stability, subcellular localization, and function of the AP-1 complex was observed in fibroblasts derived from a patient carrying an *AP1S2* mutation. Similarly, neither macro- nor microscopic defects were observed in the brain of an affected fetus. Altogether, these data suggest that the absence of an AP-1 defect in peripheral tissues is due to functional redundancy among AP-1 σ subunits (σ1A, σ1B, and σ1C) and that the phenotype observed in our patients results from a subtle and brain-specific defect of the AP-1-dependent intracellular protein traffic. Hum Mutat 29(7), 966–974, 2008. **© 2008 Wiley-Liss, Inc.**

KEY WORDS: mental retardation; clathrin; adaptor protein complex 1; AP-1; cerebral calcifications; elevated CSF protein levels; *AP1S2*

INTRODUCTION

Mental retardation (MR) is defined as cognitive functions significantly below average, associated with deficits in adaptive behavior. With a prevalence of about 2%, MR is the most common cause for referral to geneticists. X-linked mental retardation (XLMR) is a group of clinically and genetically heterogeneous conditions and has been subdivided into nonsyndromic (or isolated) forms and syndromic forms, in which the cognitive deficit is associated with specific clinical, radiological, or biochemical signs. In most cases, however, it is difficult to clinically recognize the disease-causing gene, especially as nonsyndromic and syndromic forms frequently overlap [Raymond and Tarpey, 2006; Ropers, 2006].

The Supplementary Material referred to in this article can be accessed at http://www.interscience.wiley.com/jpages/1059-7794/suppmat.

Received 22 August 2007; accepted revised manuscript 15 January 2008.

*Correspondence to: Laurence Colleaux, INSERM U781, Hôpital Necker-Enfants Malades, Tour Lavoisier, 149 Rue de Sèvres, 75015 Paris, France. E-mail: colleaux@necker.fr

Grant sponsors: Centre National de la Recherche Scientifique (CNRS); Agence Nationale de la Recherche (ANR); Association pour la Recherche sur le Cancer (ARC); Deutsche Forschungsgemeinschaft (DFG).

Guntram Borck and Anahi Mollà-Herman contributed equally to this work.

DOI 10.1002/humu.20531
Published online 21 April 2008 in Wiley InterScience (www.interscience.wiley.com).

Recently, two groups have identified mutations in the *AP1S2* gene (MIM♯ 300629) encoding σ1B, a small subunit of the clathrin-associated adaptor protein complex (AP)-1 [Tarpey et al., 2006; Saillour et al., 2007]. Affected males had mild-to-profound MR, hypotonia early in life, delayed walking, speech delay, and aggressive behavior [Carpenter et al., 1999; Turner et al., 2003; Tarpey et al., 2006; Saillour et al., 2007]. Interestingly, patients from 1 of the 5 families had been diagnosed with Fried syndrome, a distinct XLMR syndrome further characterized by basal ganglia calcifications, hydrocephalus, and spasticity [Fried, 1972; Strain et al., 1997; Saillour et al., 2007].

The clathrin-associated adaptor protein complexes AP-1 to AP-4 play key roles in the transport of proteins between intracellular organelles of the post-Golgi network, namely between the trans-Golgi network and endosomes (AP-1), the plasma membrane (AP-2), and lysosomes (AP-3 and AP-4) [Nakatsu and Ohno, 2003; Robinson, 2004]. The heterotetrameric AP complexes share a conserved structural organization and are composed of four subunits (Supplementary Fig. S1; available online at http://www.interscience.wiley.com/jpages/1059-7794/suppmat): two large subunits or adaptins (~100 kD; α-ε/β1–4), one medium (~50 kD; μ1–4), and one small subunit (~17 kD; σ1–4) [Boehm and Bonifacino, 2002]. In addition, the AP complexes share similar functions, such as assembly of clathrin coats onto target membranes and cargo selection through direct or indirect interaction with sorting signals present in the cytoplasmic domains of cargo proteins. While the role of the large and medium subunits have been extensively studied, the functions of the small σ subunits remain largely unknown [Takatsu et al., 1998]. Yet, triple-hybrid experiments have recently shown that σ subunits from AP-1, AP-2, and AP-3 interact with one of the respective large subunits to recognize leucine-based sorting signals present in the cytoplasmic tails of cargo proteins [Janvier et al., 2003; Chaudhuri et al., 2007; Doray et al., 2007].

The AP-1 complex is involved in the trafficking of cargo between the trans-Golgi network and endosomes. It is composed of two large adaptin subunits (γ and β1), a medium subunit (μ1), and a small subunit (σ1) (Supplementary Fig. S1A). There is a single gene encoding the AP-1 σ subunit in *S. cerevisiae*, *C. elegans*, and *D. melanogaster*, but there are three σ1-encoding genes in mouse and human: *AP1S1*, *AP1S2*, and *AP1S3*, encoding the σ1A, σ1B, and σ1C subunits, respectively. The *AP1S2* gene maps to chromosome Xp22.2 and encodes σ1B, a 157–amino acid protein.

Here, we report two novel families with *AP1S2* mutations. Clinical data show that *AP1S2* mutations result in a recognizable XLMR syndrome. Moreover, we present functional analyses of an *AP1S2* nonsense mutation that shed new light on the role of *AP1S2*/σ1B in the stability and function of the AP-1 complex.

SUBJECTS AND METHODS

Clinical Reports

Family 1. The propositus (Patient 1; III.1, Fig. 1A) was born to unrelated French parents after a normal pregnancy (birth weight 3,210 g, length 48 cm, and occipitofrontal circumference [OFC] 34 cm). Hypotonia was present in the first years of life and he was described as a calm and passive baby. He sat at 18 months and walked at 2 years. There was a marked speech delay, with his first words spoken at 7 years. He had hypermetropia and a small penis. He had profound MR with a developmental age between 2.4 years (cognition) and 4.6 years (fine motor skills) at a chronological age of 15.7 years, as assessed by the psychoeducational profile-revised scale (PEP-R). He had a normal stature and relative microcephaly (OFC between −0.5 and −2 standard deviations [SD]) and developed obesity. At age 20 years, his height was 173 cm (mean), weight 91 kg (+4 SD), and OFC 55 cm (–0.5 SD). He had stereotypic hand movements, repetitive activities, poor eye contact, and no social contacts. He had very limited speech, with echolalia. In the autism diagnostic interview-revised (ADI-R), his subscores for socialization, communication, and stereotyped behaviors were 24, 14, and 3, respectively, consistent with autism spectrum disorder (ASD).

His younger brother (Patient 2; III.4) was born with a birth weight of 3,170 g, length of 50 cm, and OFC of 34 cm. He was hypotonic and had feeding problems. He sat at 15 months and walked at 2 years. He said two words at 1 year of age but his subsequent speech development was very poor. At 8 years of age, his height was 120 cm (−1 SD), weight 20 kg (−1.5 SD), and OFC 50 cm (−1.5 SD). He had a supernumerary nipple and was hypermetropic. He had profound MR with a developmental age between 5 months (cognition) and 15 months (gross motor skills) at a chronological age of 3.3 years (PEP-R). Poor eye contact, stereotypic movements of the hands, no play, and echolalia with no meaningful speech were noted. He had episodes of aggressiveness. Based on these observations and the results of the ADI-R, a Diagnostic and Statistical Manual of Mental Disorders (DSM)-IV diagnosis of ASD was made. ADI-R subscores were significant in the three domains: socialization subscore 24, communication subscore 14, and stereotyped behaviors subscore 8.

Their maternal uncle (Patient 3; II.4) had reportedly profound MR. As an adult, he was not toilet trained, had no communication, and was dependent in most daily activities including eating and dressing. He lives in an institution for the mentally handicapped.

Based on the molecular results described below, prenatal diagnosis was offered to individual II.5. The male fetus carried the disease-associated haplotype and the couple elected, after counseling, to terminate the pregnancy at 20 weeks of gestation.

Family 2. Patient 4 (II.2, Fig. 1B) was born at term with normal growth parameters (weight 3,180 g, length 48 cm, and OFC 34.5 cm) to unrelated French parents. He had muscular hypotonia during the first 2 years of life, developmental delay with psychomotor regression, and a decline in OFC centile. He developed behavioral problems with aggressive outbursts. There was also delay in the onset of speech but he subsequently learned to speak fluently. However, he was not able to read, write, or count at age 11 years. At this age, his height was 127 cm (−2.5 SD), weight 27 kg (−1 SD), and OFC 49 cm (−2.5 SD). There was no facial dysmorphism. He had bilateral clinodactyly of the fifth finger and a single café-au-lait spot. At age 12 years, he presented severe MR with an intelligence quotient (IQ) of 46 (verbal IQ = 53, performance IQ = 46).

None of the patients had a history of seizures.

In several affected individuals, the following tests showed normal results: karyotype at 500-band resolution, search for fragile X syndrome, electroencephalography, and routine biochemical tests, including serum protein and calcium. Cerebral magnetic resonance imaging (MRI) was normal in Patients 1 and 4. No lactate peak was observed on magnetic resonance spectroscopy in Patient 1. Positron emission tomography was performed in Patient 2 and showed normal cerebral blood flow, including in the basal ganglia. None of the affected individuals had white matter anomalies on MRI. Results of cerebral imaging of Patient 3 are not known.

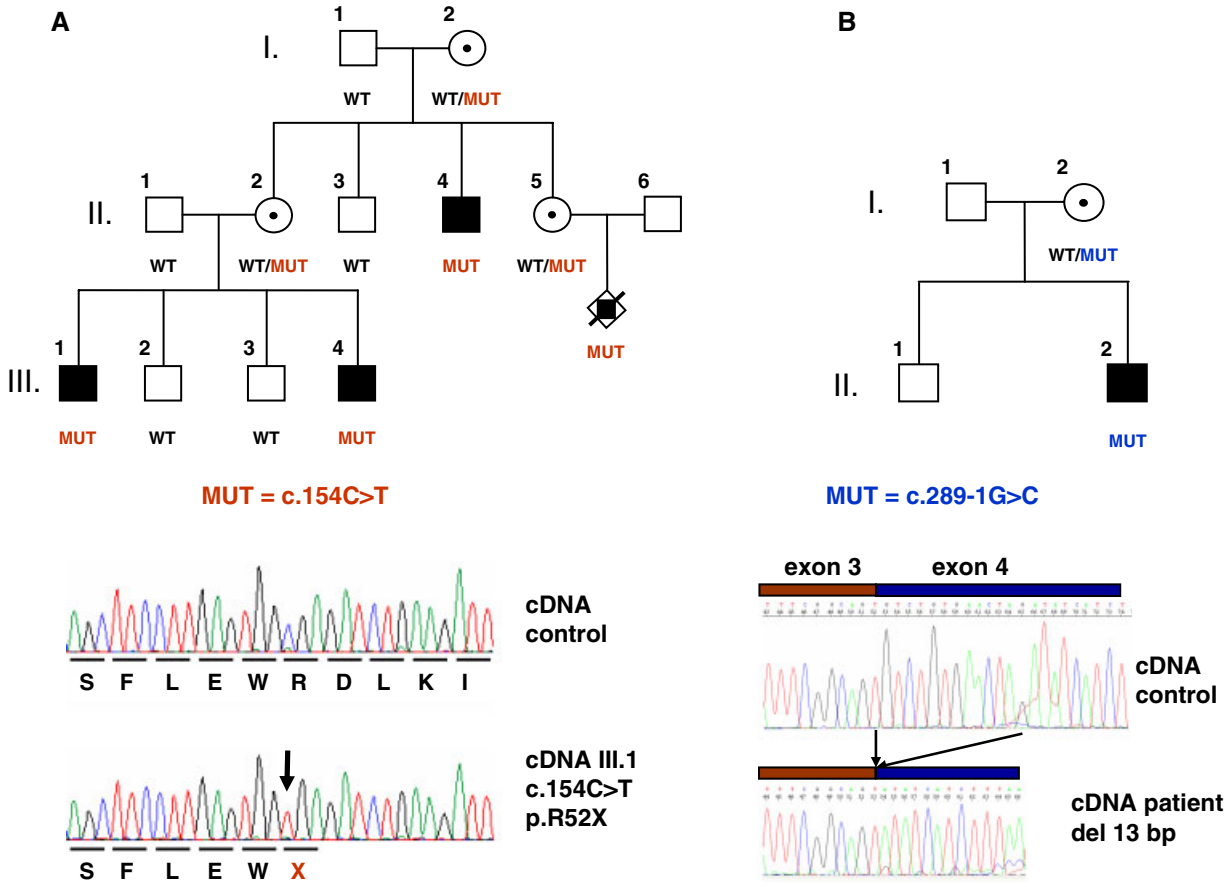

FIGURE 1. **Identification and characterization of *AP1S2* mutations. A: (top) Pedigree of Family 1. Patients 1, 2, and 3 are individuals III.1, III.4, and II.4, respectively. The c.154C>T (p.R52X) mutation (MUT) cosegregates with MR in the family WT, wild-type. A: (bottom) Electropherograms showing a wild-type sequence and the c.154C>T (p.R52X) mutation amplified from control and patient fibroblast cDNA, respectively. B: (top) Pedigree of Family 2. The affected boy (II. 2, represented by a black square) is Patient 4. B: (bottom) Sequence electropherograms showing normal splicing in a control, whereas a deletion of the first 13 base pairs of exon 4 is found in Patient 4. Sequencing was performed on cDNA reverse-transcribed from fresh blood RNA. [Color figure can be viewed in the online issue, which is available at www.interscience.wiley.com.]**

Elevated cerebrospinal fluid (CSF) protein levels were first incidentally found in Patient 2 on CSF analysis performed to rule out meningitis during an acute illness. CSF was then controlled twice after resolution of the symptoms. The first lumbar puncture in Patient 4 had been performed because a diagnosis of lysosomal storage disease had been considered.

No CSF analysis was performed in Patients 1 and 3.

Molecular Analyses

Written informed consent was obtained from the parents of subjects participating in the study.

We performed linkage analysis using 18 highly polymorphic X-chromosomal microsatellite markers. Additional markers were then selected in the candidate region and genotyped in all members of Family 1. Candidate genes were sequenced on genomic DNA of one affected boy. Based on the genomic sequence, four primer pairs were designed for PCR amplification of coding exons and splice sites of the *AP1S2* gene (reference sequence NM_003916.3). Nomenclature of the mutations is based on their respective position in the *AP1S2* mRNA sequence with the A of the translation initiation codon, which is located in exon 2, being nucleotide+1. Primers and PCR conditions are available on request. PCR products were purified with Exo-SAP (Amersham Biosciences, Orsay, France; www.amersham.com) and directly sequenced on an ABI PRISM 3130 DNA Sequencer (Applied Biosystems [ABI], Courtaboeuf, France; www.appliedbiosystems.com) using the dye terminator method according to the manufacturer's instructions.

Total RNA was extracted from cultured fibroblasts (Patient 1), or from fresh blood (Patient 4) using the PureLink Total RNA Blood Purification Kit (Invitrogen, Cergy Pontoise, France; www.invitrogen.com).

X chromosome inactivation patterns in carrier females were determined on genomic DNA extracted from white blood cells using the androgen receptor (human androgen receptor gene [HUMARA]) assay as previously described [Allen et al., 1992].

Cells, Antibodies, Western Blot, and siRNA

HeLa cells (ATCC, Manassas, VA; www.atcc.org), RPE1 cells (kind gift of M. Bornens, Institut Curie, Paris, France), and fibroblasts were grown in DMEM supplemented by 10% fetal bovine serum (Invitrogen).

Rabbit polyclonal antibody M-300 against the α-adaptin subunit of AP-2 was from Santa Cruz Biotechnology (Santa Cruz, CA; www.scbt.com), mouse monoclonal antibodies 100.3 and rabbit polyclonal antibody against the γ-adaptin subunit of AP-1 were from Santa Cruz Biotechnology and Sigma (St. Louis, MO; www.sigmaaldrich.com). Rabbit polyclonal antibodies against μ1A

(Ry/1) and σ1A (DE/1) were kindly provided by Dr. L. Traub (University of Pittsburgh School of Medicine, Pittsburgh, PA) [Traub et al., 1995; Zhu et al., 1998]. To our knowledge, no antibody specific for the σ1B subunit is available. Rabbit polyclonal antibody against σ2 (AP17) was kindly provided by Dr. M.S. Robinson (Medical Research Council [MRC], Cambridge, UK) [Page and Robinson, 1995].

Mouse monoclonal antibody 22D4 against the cation-dependent mannose 6 phosphate receptor (CD-M6PR) [Messner, 1993] was kindly provided by Jack Rohrer (University of Zürich, Zürich, Switzerland). Mouse monoclonal antibody against γ-tubulin (GTU-88) was from Sigma. Alexa594- and Alexa 488-labeled donkey anti-rabbit and donkey anti-mouse secondary antibodies were from Molecular Probes (Invitrogen).

Proteins were extracted from fibroblasts derived from skin biopsies of Patient 1 and a male control or from small interfering RNA (siRNA)-treated HeLa cells. A total of 40 μg (fibroblasts) or 25μg (HeLa cells) μg of total protein extracts were used for Western blot analyses on 10% or 12% acrylamide gels.

For siRNA treatment, HeLa or RPE1 cells were transfected with the previously described siRNA duplex (Dharmacon, Lafayette, CO; www.dharmacon.com) specific for the human α-adaptin or μ2 subunit of AP-2 or luciferase (control) with Oligofectamine (Invitrogen) according to the manufacturer's instructions and to the protocol developed by Motley et al. [2003] (α-adaptin siRNA: 5′-AUG GCG GUG GUG UCG GCU CTT-3′; μ2 siRNA: 5′-AAG UGG AUG CCU UUC GGG UCA-3′, Luciferase siRNA: 5′-CGU ACG CGG AAU ACUU CGA TT-3′). For the targeting of the σ2 subunit of AP-2, a smart pool from Dharmacon (ON-target plus SMART pool L-011833-01-0005) was transfected following the same protocol. Briefly, 200 pmol of siRNA were transfected the first day. On the second day, cells were washed twice in PBS and again transfected with 200 pmol of siRNA. Cells were processed for immunofluorescence (IF) or biochemistry two days after the second round of siRNA.

IF Analyses

For IF experiments, cells were grown directly on coverslips and processed as previously described [Montagnac et al., 2005; Burtey et al., 2007] except for siRNA-treated RPE1 or HeLa cells, which were trypsinized the day before and then grown on coverslips coated with poly-lysine (Sigma). Cells were washed in PBS and fixed in methanol at −20°C for 4 min or in 3.7% paraformaldehyde (PFA) 0.03 M sucrose for 30 min at 4°C. The cells were then incubated with primary antibodies in permeabilization buffer (PBS supplemented with 1 mg/ml BSA and 0.1% triton X-100) for 45 min at room temperature. After two washes with PBS 1 mg/ml BSA, cells were incubated for 45 min at room temperature in PBS 1 mg/ml BSA containing secondary antibodies. After two washes in permeabilization buffer and one in PBS, the cells were mounted on microscope slides using the slow fade reagent kit with DAPI (Invitrogen).

Samples were examined under an epifluorescence microscope (Leica Microsystems, Rueil-Malmaison, France; www.leica-microsystems.com) with a cooled CCD camera (Micromax; Roper-Scientific, Evry, France; www.roperscientific.com). Images were acquired with MetaMorph (Molecular Devices, Downingtown, PA; www.moleculardevices.com) and processed with MetaMorph, NIH image, or Image J (rsb.info.nih.gov/nih-image) and PhotoShop (Adobe Systems, San Jose, CA; www.adobe.com).

Immunostaining of fetal brain was performed on PFA-fixed paraffin-embedded 7-μm samples using a synaptophysin antiserum.

RESULTS

Molecular Analyses

Three males in two generations were affected by XLMR in Family 1 (Table 1; Fig. 1A). Genotype analyses performed with microsatellite markers spanning the X chromosome indicated linkage to an 18.6-Mb interval on Xp22.2−p21.1 between markers DXS987 and DXS1243 (data not shown). We first excluded five known XLMR genes mapping to this region, namely *ARX*, *IL1RAPL1*, *RPS6KA3/RSK2*, *CDKL5/STK9*, and *SMS*. The *AP1S2* gene was then regarded as a strong candidate by both localization and clinical overlap of affected family members with recently reported patients harboring mutations in this gene [Tarpey et al., 2006; Saillour et al., 2007].

Molecular analysis of the *AP1S2* gene on genomic and complementary DNA detected a c.154C>T mutation in exon 2 in Patient 1 (Fig. 1A). This mutation cosegregated with the disease in Family 1. Patients 1–3 were hemizygous and the obligate carriers I.2 and II.2 as well as individual II.5 were heterozygous for the mutation, whereas three unaffected males received the wild-type allele. The same mutation was detected in a male fetus carrying the disease-associated haplotype (Fig. 1A). The c.154C>T mutation affects a hypermutable CpG dinucleotide and predicts a p.R52X nonsense substitution that has been previously identified in an unrelated family, MRX59 (MIM# 300630) [Carpenter et al., 1999; Tarpey et al., 2006]. Neither gross alteration of *AP1S2* expression nor abnormal RNA splicing were observed in cultured fibroblasts of Patient 1.

Patient 4 is an affected boy unrelated to Family 1. Clinical similarities with Patient 2, i.e., MR, hypotonia in infancy, delayed walking, calcifications of the basal ganglia, and elevated CSF protein levels, prompted us to diagnose him with the same disorder. Sequencing of the *AP1S2* gene confirmed this diagnosis as we identified a novel mutation within the acceptor splice-site of exon 4 in Patient 4 (c.289–1G>C). His clinically unaffected mother was heterozygous for the mutation (Fig. 1B). In silico analysis using the NNSPLICE software (www.fruitfly.org/seq_tools/splice.html) predicted a complete loss of the acceptor splice-site recognition. Consistently, analysis of the *AP1S2* transcript from fresh blood cells revealed a splicing defect with three abnormal transcripts predicting truncated proteins in Patient 4. The major transcript harbored a deletion of the first 13 bp of exon 4 (Fig. 1B) caused by the use of a cryptic acceptor splice-site located downstream of the mutation. This deletion was predicted to cause a frameshift followed by a premature stop codon (p.Val97fsX55). Two minor transcripts corresponded to the skipping of exon 3 (109 bp) and exons 3−4 (247 bp; not shown).

Neither of the two mutations was found in 726 control alleles in a previous study [Tarpey et al., 2006].

Clinical Presentation

Cranial computerized tomography (CT) scanning detected bilateral calcifications of the basal ganglia in three patients (Fig. 2). Interestingly, our data provide two lines of evidence for a delayed occurrence of these calcifications in childhood. First, no calcification was observed on histological brain sections of the affected fetus after termination of pregnancy at 20 weeks of gestation (see below). Second, based on iterative CT scans, calcifications appeared between 1 and 9 years of age in Patient 2 (Fig. 2A and B).

While calcifications were confined to the head of the caudate nucleus and to parts of the pallidum in Patient 2 at 9 years (Fig. 2B) and to the entire caudate nucleus in Patient 4 at 14 years

TABLE 1. Clinical Phenotype of Patients Harboring an *AP1S2* Mutation

	This report, Patients 1–3 (n = 3)	This report, Patient 4 (n = 1)	Tarpey et al. [2006], Family 63 (n = 4)	Turner et al. [2003], Family 445 (n = 7)	Carpenter et al. [1999], MRX59 (n = 5)	Saillour et al. [2007] (n = 5)	Fried [1972] and Strain et al. [1997] (n = 8)	Total (n = 33)
AP1S2 mutation[a]	c.154C>T (p.R52X)[b]	c.289–1G>C[c]	c.180-5_180-1del4 [Tarpey et al., 2006]	c.106C>T (p.Q36X) [Tarpey et al., 2006]	c.154C>T (p.R52X) [Tarpey et al., 2006]	c.288+5G>A [Saillour et al., 2007]	c.226G>T (p.Q66X) [Saillour et al., 2007]	
Type of mutation	Nonsense	Splice site	Splice site	Nonsense	Nonsense	Splice site	Nonsense	4 Nonsense; 3 splice site
Mean birth weight in g (range)	3,190 (n = 2) (3,170–3,210)	3,180	NA	3,425 (n = 4) (3,000–3,850)	3,136 (n = 5) (2,440–3,520)	3,555 (n = 2) (3,460–3,650)	3,600 (n = 1)	3,310 (n = 15) (2,440–3,850)
MR	Profound	Severe	Mild-profound	Mild-moderate	Mild-profound	Borderline-profound	Severe-profound	Borderline-profound
Microcephaly	0/2	1/1	0/4	6/7	2/5	NA	1/5	10/24
Short stature	0/2	1/1	NA	2/6	0/5	NA	2/3	5/17
Hypotonia	2/2	1/1	4/4	7/7	5/5	5/5	1/1	25/25
Delay in walking	3/3	1/1	3/3	4/5	5/5	2/3	2/?	18/20
Abnormal speech[d]	3/3	1/1	2/4	7/7	3/5	2/2	2/?	18/22
Aggressive behavior	1/2	1/1	1/4	5/7	3/5	1/3	NA	12/22
Seizures	0/3	0/1	1/4	1/7	0/5	1/5	0/8	3/33
Cerebral calcifications	2/2	1/1	NA	NA	NA	2/2	2/2	7/7
ASD	2/2	0/1	NA	NA	NA	NA	NA	2/3
Elevated CSF protein levels	1/1	1/1	NA	NA	NA	NA	NA	2/2

[a]Nomenclature of the mutations is based on their respective position in the *AP1S2* mRNA sequence (reference sequence NM_003916.3) with the A of the translation initiation codon, which is located in exon 2, being nucleotide+1.
[b]Same mutation previously identified in unrelated family MRX59 [Tarpey et al., 2006].
[c]Novel mutation.
[d]Abnormal speech is defined as speech delay and minimal or absent speech.
ASD, autism spectrum disorder; CSF, cerebrospinal fluid; MR, mental retardation.

(Fig. 2C), they were more widespread in the older patient (Patient 1 at 20 years), extending bilaterally to the caudate nucleus and the pallidum (Fig. 2D and E). These results show that cerebral calcifications appear in childhood and suggest that they are progressive. We observed a moderate signal enhancement of the basal ganglia after injection of contrast medium on CT scan of Patient 1 (Fig. 2E and F). One boy had bilateral dilatation of the lateral ventricles and the subarachnoid spaces that subsequently resolved spontaneously, giving place to slit ventricles (Fig. 2G and H).

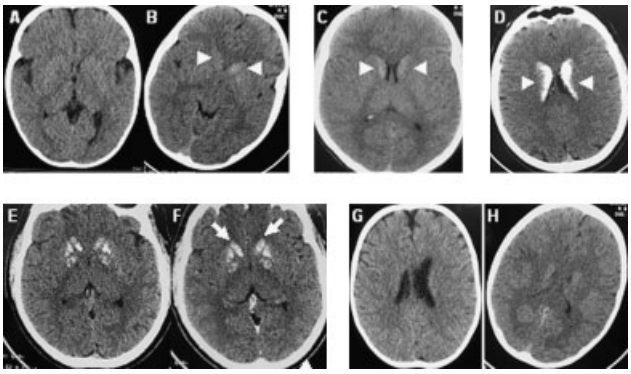

FIGURE 2. **Evidence of calcifications of the basal ganglia. Axial brain CT scans of Patient 2 (A,B,G,H), Patient 4 (C) and Patient 1 (D,E,F). Calcifications are highlighted by arrowheads. No cerebral calcifications were seen in Patient 2 at 1 year of age (A), but calcifications were visible at 9 years (B). Calcifications in Patient 4 at 14 years (C) and in Patient 1 at 20 years (D). CT scan of Patient 1 without (E) and with injection of contrast medium (F) showing a moderate postinjection enhancement of the caudate nuclei (arrows) consistent with a disruption of the blood-brain barrier. G: Enlarged lateral ventricles and subarachnoid spaces in Patient 2 at 1 year of age. These enlargements have disappeared eight years later (H).**

In addition, elevated CSF protein levels were repeatedly found in the two patients who underwent lumbar puncture. Indeed, CSF protein levels were approximately twice higher than the upper limit of normal (Patient 2: 0.81 g/l and 0.95 g/l at 1 year and 2.5 years of age, respectively (normal < 0.45 g/l); Patient 4: 1.12 g/l and 1.02 g/l at 16 months and 6 years of age, respectively). CSF glucose and cells were normal and there were no signs or symptoms of an acute or chronic infectious, inflammatory, or demyelinating disease.

Heterozygous carriers were considered to be unaffected. However, it is worth noting that individual II.2 (Family 1) underwent ventriculoperitoneal shunt operation for hydrocephalus at age 39 years. Analysis of the methylation pattern at the androgen receptor gene locus showed that her X chromosome inactivation pattern was 89:11 whereas it was 51:49 in the mother of Patient 4.

Biochemical and Functional Analyses of AP Complexes

Considering that inactivation of various AP-1 subunits leads to destabilization of the remaining subunits of the complex in model organisms [Zizioli et al., 1999; Meyer et al., 2000] and in vitro, using siRNA [Hirst et al., 2003; Janvier and Bonifacino, 2005], we first investigated the consequences of the *AP1S2* p.R52X mutation on the integrity of the AP-1 complex in fibroblasts by IF using an anti-AP-1 γ-adaptin antibody. As a control, the distribution of the AP-2 complex was tested in the same cells by IF using an anti-AP2 α-adaptin antibody. The AP-2 complex showed a punctate staining pattern in patient and control fibroblasts, corresponding to plasma membrane clathrin-coated pits (CCPs) (Fig. 3A and B). As far as

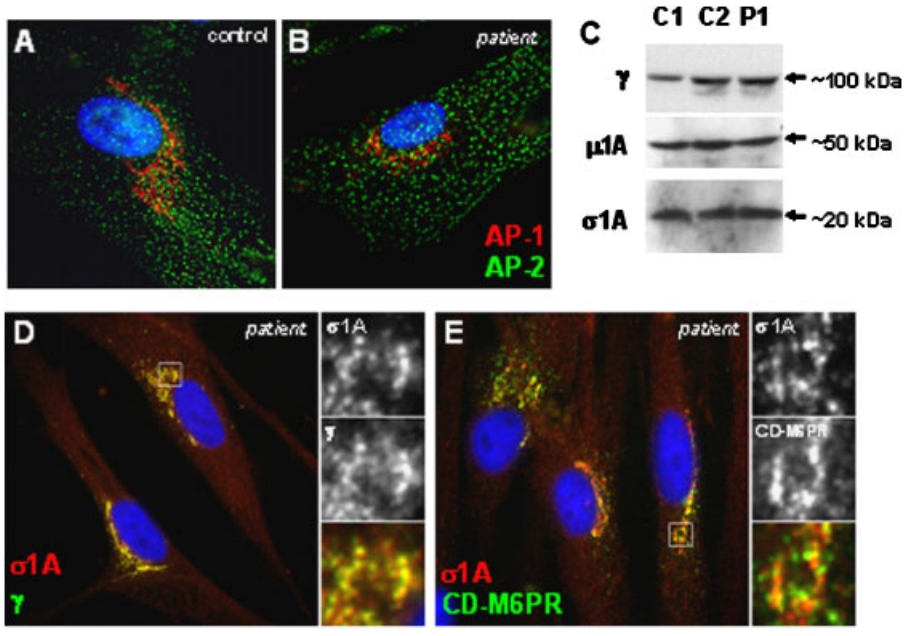

FIGURE 3. **AP-1 complex in *AP1S2*/σ1B-deficient cells. Control (A) and patient fibroblasts (B) were stained for AP-2 (α subunit, green) and AP-1 (γ subunit, red) complexes as described in Subjects and Methods. Lysates of control and patient fibroblasts were subjected to Western blotting for GAPDH as a loading control (not shown) and for AP-1 subunits using anti-γ, -μ1A, and -σ1A subunit antibodies (C). Antibodies are indicated on the left and molecular weights on the right. C, control; P1, Patient 1. Distributions of AP-1 complex subunits γ (green) and σ1A (red; D) and of AP-1 (σ1A, red) and the cation-dependent mannose 6 phosphate receptor (CD-M6PR, green; E) were analyzed by IF. A representative area (white squares) was enlarged (× 3) to show colocalization of the markers (D and E, right column). Nuclei were stained with DAPI (blue).**

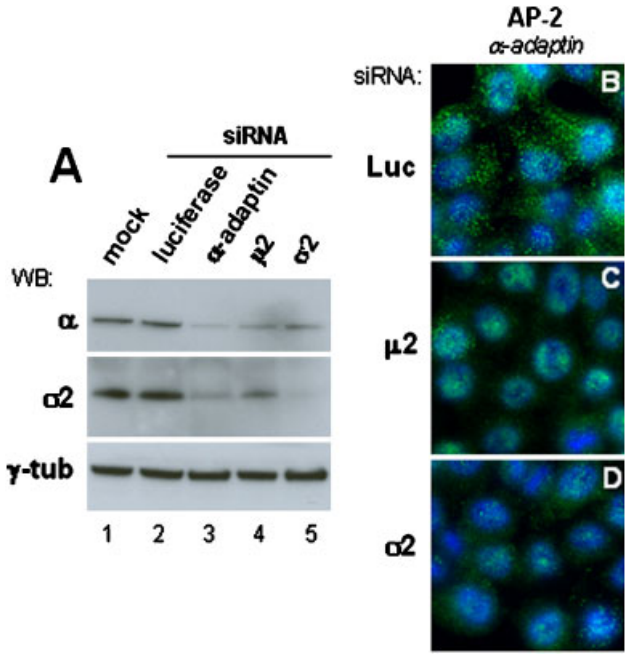

FIGURE 4. **Destabilization of the AP-2 complex in σ2-deficient HeLa cells. (A) Control HeLa cells (lane 1) or HeLa cells treated with control siRNA (luciferase; lane 2) or siRNA targeting AP-2 subunits (α-adaptin, μ2, and σ2; lanes 3, 4, and 5, respectively) were analyzed by Western blot using antibodies against α-adaptin, σ2, or γ-tubulin as indicated. HeLa cells treated with luciferase (LUC) (B), μ2 (C), or σ2 (D) siRNA were fixed and stained for AP-2 α-adaptin subunit (green). Nuclei were stained with DAPI (blue). WB, Western blot; γ-tub, γ-tubulin.**

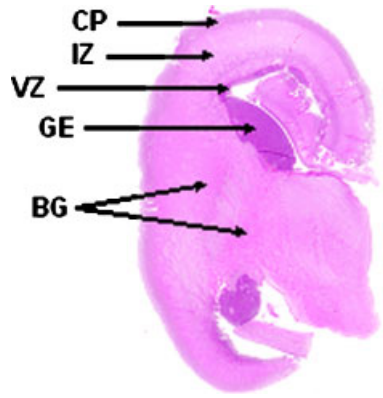

FIGURE 5. **Brain morphology of a fetus carrying an *AP1S2* nonsense mutation. Coronal section (hematein-eosin staining) of brain hemispheres at the level of the basal ganglia. Note normal brain morphology and absence of calcifications. Calcifications would manifest as dark blue areas using this staining. BG, basal ganglia; CP, cortical plate; GE, ganglionic eminence; IZ, intermediate zone; VZ, ventricular zone.**

AP-1 is concerned, γ-adaptin staining showed a similar reticulated juxtanuclear distribution corresponding to the trans-Golgi network in control and patient fibroblasts (Fig. 3A and B), suggesting that the stability of the AP-1 complex was not affected by the *AP1S2* mutation. Consistently, Western blot analyses showed that the γ and μ1A subunits were expressed at similar levels in patient and control fibroblasts (Fig. 3C). Taken together, these results suggest that, at least in this cell type and under the experimental conditions tested, the *AP1S2* mutation does not compromise the stability of the AP-1 complex.

While no AP1S2/σ1B-specific antibodies are available, Western blot experiments using anti-σ1A antibodies showed that AP1S1/σ1A was expressed at similar levels in control and patient fibroblasts (Fig. 3C) and that AP1S1/σ1A colocalized with γ-adaptin in patient fibroblasts (Fig. 3D), suggesting that patient fibroblasts assemble functional AP-1 complexes containing σ1A subunits. We also tested the effect of the *AP1S2* mutation on the distribution of the cation-dependent mannose-6-phosphate receptor (CD-M6PR), a known AP-1 cargo protein. In the absence of a functional AP-1 complex in mice deficient for the AP-1 μ1A subunit, CD-M6PR has been shown to mislocalize into endosomes [Meyer et al., 2000]. The distribution of CD-M6PR was similar in patient and control fibroblasts and CD-M6PR colocalized with AP-1 at the trans-Golgi network (Fig. 3E; data not shown), indicating that the AP-1 dependent trafficking of CD-M6PR was not affected in *AP1S2*/σ1B mutant fibroblasts.

Targeting of individual AP-1–4 subunits in human cell lines using specific siRNA has shown that depletion of either large adaptin (α, γ, δ) or medium subunits (μ1–4) results in destabilization of the whole complex [Hirst et al., 2003; Motley et al., 2003; Janvier and Bonifacino, 2005]. Surprisingly, RNA inhibition of the small (σ) subunits on AP stability has never been investigated. Unfortunately, our attempts to knock down *AP1S1*/σ1A by siRNA in cultured control and patient fibroblasts failed. To gain further insight into the role of σ subunits in AP complexes, we decided to use the AP-2 complex as a model system because its σ subunit (σ2) is encoded by a single gene (*AP2S1*) (Supplementary Fig. S1B). We compared the effect of anti-AP-2 σ2 siRNA to that of anti-AP-2 μ2 or α siRNA, both of which have been shown previously to affect the integrity of the whole complex [Motley et al., 2003], by Western blot (Fig. 4A) and IF (Fig. 4B–D; Supplementary Fig. S2). While no anti-σ2-antibody suitable for IF analyses was available, Western blot experiments showed that anti-σ2 siRNA caused a strong decrease of σ2 protein in HeLa cells compared to control cells while γ-tubulin expression was not affected (Fig. 4A), thereby demonstrating the efficiency and specificity of this siRNA. As expected, decrease of σ2 protein was also observed in cells treated with either anti-α or anti-μ2 siRNA (Fig. 4A, lanes 3 and 4). Interestingly, depletion of σ2 also resulted in a decreased expression of α-adaptin (Fig. 4A, lane 5; Supplementary Fig. S2) demonstrating that, as previously observed for α and μ2 subunits, depletion of the σ2 subunit causes destabilization of the other AP-2 subunits. Notably, anti-σ2 siRNA caused a loss of AP-2 punctate staining at the plasma membrane in two cell lines, HeLa (Fig. 4D) and RPE1 (Supplementary Fig. S2), with an efficiency similar to that observed with anti-μ2 siRNA (Fig. 4C; Supplementary Fig. S2). This effect was specific of the AP-2 complex as siRNA targeting of AP-2 subunits did not affect AP-1 in the same cells (Supplementary Fig. S2). Altogether, these results indicate that targeting the unique σ2 gene affects AP-2 stability.

Neuroanatomical Consequences of the p.R52X Mutation

Autopsy of the aborted male fetus in Family 1 carrying the c.154C>T (p.R52X) mutation showed normal fetal biometry and normal macro- and microscopic brain morphology. Moreover, no cerebral calcifications were observed upon macroscopic inspection, on histological sections (Fig. 5), and microscopically, at low and high magnification (data not shown).

Because the AP-1 γ-subunit has been shown to interact with synaptophysin [Horikawa et al., 2002], we performed immunohistochemistry with an anti-synaptophysin antibody on brain sections of the affected fetus and a control matched for sex and gestational age. No significant qualitative differences in synaptophysin immunostaining were found throughout the brain (data not shown).

DISCUSSION

The patients reported here share many features with those recently reported by others [Tarpey et al., 2006; Saillour et al., 2007]. Normal growth parameters at birth, hypotonia in infancy, delayed walking, and speech delay with subsequent absent or minimal language have been reported in most patients. Aggressive behavior and microcephaly (defined as OFC < -2 SD [Mochida and Walsh, 2001]) are also observed (Table 1). Remarkably, MR ranges from mild to profound and the severity of language deficit is also variable, as Patient 4 (this report) had fluent and meaningful language and had learned a foreign language. In addition, the two affected siblings in Family 1 have been diagnosed with ASD based on the ADI-R. As Patient 4 was diagnosed with the same syndrome as Patient 2 based on clinical features alone, our results show that *AP1S2* mutations are responsible for a clinically recognizable XLMR and autism syndrome initially described as Fried syndrome.

We show here that *AP1S2* mutations are associated with elevated CSF protein levels, a feature that has not been observed before. Only a few XLMR disorders have been described in which a laboratory or neuroradiological investigation can help making the diagnosis, namely XLMR due to mutations in the *SLC6A8*, *SLC16A2/MCT8*, *SMS*, and *ACS4/FACL4* genes. Our findings suggest that the finding of an unexplained elevation of CSF protein in a mentally retarded boy should prompt a molecular analysis of the *AP1S2* gene. The pathophysiology leading to elevated protein levels in CSF remains unclear at this stage. Because an electrophoresis of CSF proteins in Patients 2 and 4 showed a high albumin concentration and no intrathecal immunoglobulin G production (data not shown), leakage of serum proteins through a defective blood-brain barrier seems a plausible explanation [Ballabh et al., 2004], which is corroborated by the moderate signal enhancement of the basal ganglia after injection with contrast medium in Patient 1.

We also observed calcifications of the basal ganglia in the three patients who underwent CT scans, thereby confirming a recent report [Saillour et al., 2007]. Similar calcifications are associated with autosomal dominant idiopathic basal ganglia calcification (IBGC1 or Fahr disease) and with autosomal recessive Aicardi-Goutières syndrome [Geschwind et al., 1999; Goutières, 2005]. While the mode of inheritance distinguishes these disorders from XLMR due to *AP1S2* mutations, they are also characterized by neurologic and psychiatric manifestations. We have shown that basal ganglia calcifications appear during childhood and might be progressive but the pathogenesis leading to calcium deposition remains unexplained and might include necrosis or vascular calcification. From a clinical point of view it is important to note that, while MRI is the method of choice for the identification of cerebral malformations and anomalies of cortical development, CT is more sensitive than MRI in detecting calcifications [Battaglia, 2003; Sato, 2003].

Two different AP-1-deficient mice have been reported, namely models for γ and μ1A subunit genes [Zizioli et al., 1999; Meyer et al., 2000]. Both γ and μ1A deficiency resulted in drastic destabilization of the AP-1 complex and were embryonic lethal, demonstrating that AP-1 is essential for viability in mammals. By contrast, *AP1S2* deficiency in human is viable and causes a phenotype restricted to the central nervous system. Our data show that in patient fibroblasts there is no alteration of the stability, subcellular localization, or function of the AP-1 complex. This suggests that in peripheral tissues, the structural role of *AP1S2*/σ1B can be performed by another σ1 subunit. Along this line, it is worth noting that σ1B (encoded by *AP1S2*) shares 87% and 79% amino acid identity with σ1A (encoded by *AP1S1*) and σ1C (encoded by *AP1S3*), respectively [Takatsu et al., 1998]. Moreover, a similar mechanism has been experimentally validated for the AP-1 medium subunits μ1A and μ1B, which share 80% amino acid identity. In fibroblasts, the epithelia-specific μ1B subunit can structurally and functionally compensate the deficiency of the ubiquitous μ1A [Eskelinen et al., 2002]. Finally, we demonstrated that depletion of the unique σ2 subunit affected the stability of the AP-2 complex. Our results, along with the observation that depletion of the unique σ1 subunit in *C. elegans* affected the stability of the other AP-1 subunits [Shim et al., 2000], clearly indicate that σ subunits are required for the stability of AP complexes.

Clathrin-coated vesicles isolated from rat brain contain (besides different AP-1 and AP-2 subunits) a large number of synaptic proteins, consistent with their role in synaptic vesicle recycling [Blondeau et al., 2004]. In addition, AP-1 has been shown to be involved in dendrite-specific trafficking in neurons in *C. elegans* [Dwyer et al., 2001]. As the only described function of σ subunits is the interaction with leucine-based sorting signals [Janvier et al., 2003; Chaudhuri et al., 2007; Doray et al., 2007], it is tempting to speculate that the phenotype observed in our patients might be related to a targeting defect of neuron specific cargo, the sorting of which would be strictly dependent on *AP1S2*/σ1B.

In summary, this study contributes to better delineate the clinical profile of *AP1S2* mutations and provides clues for a better understanding of the pathophysiological consequences of these mutations. Elevated CSF protein and cerebral calcifications could be regarded as diagnostic criteria of this syndrome. The brain-specific phenotype observed in our patients might be due to the disruption of the cellular sorting of a specific subset of synaptic proteins and to the redundancy of σ1 subunits in peripheral tissues.

ACKNOWLEDGMENTS

We are grateful to the families for their participation in the study. We thank Florence Molinari, Charles Schwartz, and André Hanauer for contributions to candidate gene screening, David Geneviève and Marlène Rio for communicating clinical information, Alice Bourdon for help with Western blots, Gregory Camus and Jérôme Bouchet for help with siRNA against AP-2, and Jack Rohrer, Linton Traub, and Margaret Robinson for providing antibodies. This work was supported by the Agence Nationale de la Recherche (ANR) (to L.C) and by the Association pour la Recherche sur le Cancer (ARC, n° 36-91) (to A.B.). G.B. was supported by the Deutsche Forschungsgemeinschaft (DFG).

REFERENCES

Allen RC, Zoghbi HY, Moseley AB, Rosenblatt HM, Belmont JW. 1992. Methylation of HpaII and HhaI sites near the polymorphic CAG repeat in the human androgen-receptor gene correlates with X chromosome inactivation. Am J Hum Genet 51:1229–1239.

Ballabh P, Braun A, Nedergaard M. 2004. The blood-brain barrier: an overview: structure, regulation, and clinical implications. Neurobiol Dis 16:1–13.

Battaglia A. 2003. Neuroimaging studies in the evaluation of developmental delay/mental retardation. Am J Med Genet C Semin Med Genet 117:25–30.

Blondeau F, Ritter B, Allaire PD, Wasiak S, Girard M, Hussain NK, Angers A, Legendre-Guillemin V, Roy L, Boismenu D, Kearney RE, Bell AW, Bergeron JJ, McPherson PS. 2004. Tandem MS analysis of brain clathrin-coated vesicles reveals their critical involvement in synaptic vesicle recycling. Proc Natl Acad Sci USA 101:3833–3838.

Boehm M, Bonifacino JS. 2002. Genetic analyses of adaptin function from yeast to mammals. Gene 286:175–186.

Burtey A, Rappoport JZ, Bouchet J, Basmaciogullari S, Guatelli J, Simon SM, Benichou S, Benmerah A. 2007. Dynamic interaction of HIV-1 nef with the clathrin-mediated endocytic pathway at the plasma membrane. Traffic 8:61–76.

Carpenter NJ, Brown WT, Qu Y, Keenan KL. 1999. Regional localization of a nonspecific X-linked mental retardation gene (MRX59) to Xp21.2-p22.2. Am J Med Genet 85:266–270.

Chaudhuri R, Lindwasser OW, Smith WJ, Hurley JH, Bonifacino JS. 2007. Downregulation of CD4 by human immunodeficiency virus type 1 nef is dependent on clathrin and involves direct interaction of nef with the AP2 clathrin adaptor. J Virol 81:3877–3890.

Doray B, Lee I, Knisely J, Bu G, Kornfeld S. 2007. The gamma/sigma1 and alpha/sigma2 hemicomplexes of clathrin adaptors AP-1 and AP-2 harbor the dileucine recognition site. Mol Biol Cell 18:1887–1896.

Dwyer ND, Adler CE, Crump JG, L'Etoile ND, Bargmann CI. 2001. Polarized dendritic transport and the AP-1 mu1 clathrin adaptor UNC-101 localize odorant receptors to olfactory cilia. Neuron 31: 277–287.

Eskelinen EL, Meyer C, Ohno H, von Figura K, Schu P. 2002. The polarized epithelia-specific mu1B-adaptin complements mu1A-deficiency in fibroblasts. EMBO Rep 3:471–477.

Fried K. 1972. X-linked mental retardation and-or hydrocephalus. Clin Genet 3:258–263.

Geschwind DH, Loginov M, Stern JM. 1999. Identification of a locus on chromosome 14q for idiopathic basal ganglia calcification (Fahr disease). Am J Hum Genet 65:764–772.

Goutières F. 2005. Aicardi-Goutières syndrome. Brain Dev 27:201–206.

Hirst J, Motley A, Harasaki K, Peak Chew SY, Robinson MS. 2003. EpsinR: an ENTH domain-containing protein that interacts with AP-1. Mol Biol Cell 14:625–641.

Horikawa HP, Kneussel M, El Far O, Betz H. 2002. Interaction of synaptophysin with the AP-1 adaptor protein gamma-adaptin. Mol Cell Neurosci 21:454–462.

Janvier K, Kato Y, Boehm M, Rose JR, Martina JA, Kim BY, Venkatesan S, Bonifacino JS. 2003. Recognition of dileucine-based sorting signals from HIV-1 nef and LIMP-II by the AP-1 gamma-sigma1 and AP-3 delta-sigma3 hemicomplexes. J Cell Biol 163:1281–1290.

Janvier K, Bonifacino JS. 2005. Role of the endocytic machinery in the sorting of lysosome-associated membrane proteins. Mol Biol Cell 16:4231–4242.

Messner DJ. 1993. The mannose receptor and the cation-dependent form of mannose 6-phosphate receptor have overlapping cellular and subcellular distributions in liver. Arch Biochem Biophys 306:391–401.

Meyer C, Zizioli D, Lausmann S, Eskelinen EL, Hamann J, Saftig P, von Figura K, Schu P. 2000. mu1A-adaptin-deficient mice: lethality, loss of AP-1 binding and rerouting of mannose 6-phosphate receptors. EMBO J 19:2193–2203.

Mochida GH, Walsh CA. 2001. Molecular genetics of human microcephaly. Curr Opin Neurol 14:151–156.

Montagnac G, Yu LC, Bevilacqua C, Heyman M, Conrad DH, Perdue MH, Benmerah A. 2005. Differential role for CD23 splice forms in apical to basolateral transcytosis of IgE/allergen complexes. Traffic 6:230–242.

Motley A, Bright NA, Seaman MN, Robinson MS. 2003. Clathrin-mediated endocytosis in AP-2-depleted cells. J Cell Biol 162:909–918.

Nakatsu F, Ohno H. 2003. Adaptor protein complexes as the key regulators of protein sorting in the post-Golgi network. Cell Struct Funct 28:419–429.

Page LJ, Robinson MS. 1995. Targeting signals and subunit interactions in coated vesicle adaptor complexes. J Cell Biol 131:619–630.

Raymond FL, Tarpey P. 2006. The genetics of mental retardation. Hum Mol Genet 15(Spec No 2):R110–R116.

Robinson MS. 2004. Adaptable adaptors for coated vesicles. Trends Cell Biol 14:167–174.

Ropers HH. 2006. X-linked mental retardation: many genes for a complex disorder. Curr Opin Genet Dev 16:260–269.

Saillour Y, Zanni G, Des Portes V, Heron D, Guibaud L, Iba-Zizen MT, Pedespan JL, Poirier K, Castelneau L, Julien C, Franconnet C, Bonthron DT, Porteous MM, Chelly J, Bienvenu T. 2007. Mutations in the AP1S2 gene encoding the sigma 2 subunit of the adaptor protein 1 complex are associated with syndromic X-linked mental retardation with hydrocephalus and calcifications in basal ganglia. J Med Genet 44:739–744.

Sato Y. 2003. Basal ganglia calcifications in childhood. Semin Pediatr Neurol 10:96–102.

Shim J, Sternberg PW, Lee J. 2000. Distinct and redundant functions of mu1 medium chains of the AP-1 clathrin-associated protein complex in the nematode *Caenorhabditis elegans*. Mol Biol Cell 11:2743–2756.

Strain L, Wright AF, Bonthron DT. 1997. Fried syndrome is a distinct X linked mental retardation syndrome mapping to Xp22. J Med Genet 34:535–540.

Takatsu H, Sakurai M, Shin HW, Murakami K, Nakayama K. 1998. Identification and characterization of novel clathrin adaptor-related proteins. J Biol Chem 273:24693–24700.

Tarpey PS, Stevens C, Teague J, Edkins S, O'Meara S, Avis T, Barthorpe S, Buck G, Butler A, Cole J, Dicks E, Gray K, Halliday K, Harrison R, Hills K, Hinton J, Jones D, Menzies A, Mironenko T, Perry J, Raine K, Richardson D, Shepherd R, Small A, Tofts C, Varian J, West S, Widaa S, Yates A, Catford R, Butler J, Mallya U, Moon J, Luo Y, Dorkins H, Thompson D, Easton DF, Wooster R, Bobrow M, Carpenter N, Simensen RJ, Schwartz CE, Stevenson RE, Turner G, Partington M, Gecz J, Stratton MR, Futreal PA, Raymond FL. 2006. Mutations in the gene encoding the sigma 2 subunit of the adaptor protein 1 complex, AP1S2, cause X-linked mental retardation. Am J Hum Genet 79:1119–1124.

Traub LM, Kornfeld S, Ungewickell E. 1995. Different domains of the AP-1 adaptor complex are required for Golgi membrane binding and clathrin recruitment. J Biol Chem 270:4933–4942.

Turner G, Gedeon A, Kerr B, Bennett R, Mulley J, Partington M. 2003. Syndromic form of X-linked mental retardation with marked hypotonia in early life, severe mental handicap, and difficult adult behavior maps to Xp22. Am J Med Genet A 117:245–250.

Zhu Y, Traub LM, Kornfeld S. 1998. ADP-ribosylation factor 1 transiently activates high-affinity adaptor protein complex AP-1 binding sites on Golgi membranes. Mol Biol Cell 9:1323–1337.

Zizioli D, Meyer C, Guhde G, Saftig P, von Figura K, Schu P. 1999. Early embryonic death of mice deficient in gamma-adaptin. J Biol Chem 274:5385–5390.